



Measurement and modeling concrete creep considering relative humidity effect

Ya Wei¹ · Jingsong Huang² · Siming Liang²

Received: 17 May 2018 / Accepted: 11 February 2019 / Published online: 19 February 2019
© Springer Nature B.V. 2019

Abstract Relative humidity plays a critical role in concrete creep. To accurately measure and model creep behavior of concrete considering the relative humidity effect is difficult despite more than 100 years of research of concrete creep. In this study, a test set-up was designed to measure the creep-induced deflection of concrete beams exposed to different drying conditions (sealed and symmetric drying). A numerical method is proposed to quantify the creep parameters of concrete considering the relative humidity effect. The sequential coupled hydromechanical finite element analysis was conducted to back-calculate the creep parameters in the microprestressing solidification theory-based creep model from the measured creep-induced deflection. It was found that the obtained parameters are independent of the loading and drying conditions. One set of parameters can predict the creep-induced deflection of concrete beams exposed to different drying conditions. The findings in this study provide a new methodology to obtain the creep parameters which can be implemented numerically for analyzing creep behavior of various concrete structures without considering the drying-related size effect.

Keywords Creep-induced deflection · Drying condition · Microprestressing solidification theory · Relative humidity effect · Sequential coupled hydromechanical analysis

1 Introduction

Creep is an intrinsic property of concrete, which affects the deformation and stress in concrete structures. The relative humidity is one of the major influencing factors to concrete creep (Acker and Ulm 2001; Cagnon et al. 2015). Concrete creeps more under drying condition than under the nondrying condition, i.e., sealed. This phenomenon is

✉ Y. Wei
yawei@tsinghua.edu.cn

¹ Key Laboratory of Civil Engineering Safety and Durability of China Education Ministry, Department of Civil Engineering, Tsinghua University, Beijing 100084, China

² Department of Civil Engineering, Tsinghua University, Beijing 100084, China

called the Pickett effect and the excess creep due to drying is usually referred to as drying creep (Pickett 1942). Over the last 70 years, several hypotheses have been proposed to explain the mechanisms of the Pickett effect (Bažant and Xi 1994; ACI 209 2008; Rossi et al. 2013). Unfortunately, no consensus has been achieved on this issue. The experimental drying creep results available in the literature are sometimes contradictory (Charron et al. 2015).

Accurately measuring and modeling concrete creep when drying is involved are still quite difficult (Sellier et al. 2016). Concrete creep was normally measured axially, either under sustained compressive or tensile load. It is unavoidable that one measure both shrinkage strain and the real creep strain during the creep test. Decoupling is often conducted to obtain the real creep strain based on the assumption that the shrinkage and the creep are additiveness. This situation becomes worse during the drying creep test, because a differential shrinkage gradient often exists in concrete specimens, and the strain might depend on the local relative humidity greatly, particularly for the surface strain measurement on a drying sample.

With respect to experimental measurement, flexural creep test has recently been used to study the creep behavior of cement-based materials (Ranaivomanana et al. 2013a; Ghezal and Assaf 2015; Un et al. 2015). For example, Ranaivomanana et al. (2013a) measured the compressive and the tensile creep strain of concrete beam at different locations by using strain gauges and found that the basic compressive creep is the same as the basic tensile creep in the bending specimens. Un et al. (2015) conducted flexural creep test on a mini-beam with size of 350 mm × 50 mm × 10 mm to study the flexural creep properties of paste and mortar under various environmental conditions. The results reveal that the flexural creep showed agreement with the general long-term uniaxial creep of cement-based materials from the literature.

Flexural creep might be an effective method to investigate concrete creep under different drying conditions since it is possible to eliminate the influence of shrinkage deformation caused by the change of relative humidity on concrete creep. In this study, both experimental and numerical methods are proposed to investigate the effect of relative humidity on concrete creep. The predicted results are then compared to the experimentally measured creep-induced deflection of concrete beams to obtain the creep parameters. To evaluate the relative humidity effect, concrete beams were exposed to sealed and symmetric drying conditions. The method to obtain the creep property considering relative humidity effect, and the measurement and verification of the predicted results are discussed in the following sections.

2 Method to obtain creep property considering relative humidity effect

2.1 Sequential coupled hygromechanical finite element analysis

Since the internal relative humidity has a great effect on concrete creep, a sequential coupled hygromechanical finite element analysis is proposed to numerically obtain the creep property considering the effect of relative humidity of concrete. The sequential coupled hygromechanical analysis is performed by first solving the pure moisture diffusion analysis, then reading the relative humidity solution into a quasi-static structural analysis. Due to the similarity of the heat transfer model and the moisture diffusion model, the module of the sequential coupled thermal-stress analysis in ABAQUS software was used to conduct the sequential coupled hygromechanical analysis. Table 1 shows the comparison of the heat

Table 1 Comparison of the heat transfer model and the moisture diffusion model in early-age concrete

Model type	Heat transfer	Moisture diffusion
Governing equation	$\rho c \frac{\partial T}{\partial t} = \nabla \cdot [k_T(T) \cdot \nabla T] + \rho c \frac{\partial T_Q}{\partial t}$	$\frac{\partial H}{\partial t} = \nabla \cdot [D(H) \cdot \nabla H] - \frac{\partial H_s}{\partial t}$
Boundary condition	$-k_T(T) \frac{\partial T}{\partial n} = \beta(T - T_{env})$	$-D(H) \frac{\partial H}{\partial n} = \lambda(H - H_{env})$

Note: T is the temperature of concrete; ρ is the density of concrete; c is the specific heat capacity of concrete; $k_T(T)$ is the thermal conductivity of concrete; $\rho c \frac{\partial T_Q}{\partial t}$ represents the generated heat of hydration per unit volume; β is the convective film coefficient; $\frac{\partial T}{\partial n}$ is the temperature gradient in direction n of concrete surface

transfer model and the moisture diffusion model in concrete. It is seen that the governing differential function and the boundary condition of these two models are quite similar to each other; it is possible to employ the module of the sequential coupled thermal-stress analysis to conduct the sequential coupled hygromechanical analysis of concrete in ABAQUS. It is noted that the couple effect of the heat transfer and moisture diffusion on concrete creep is not considered during the sequential coupled hygromechanical analysis due to the fact that the environmental temperature was controlled and kept nearly constant during the creep measurement and therefore the temperature effect can be ignored for simplicity.

In the moisture diffusion analysis, since both the diffusion from external drying and the self-desiccation from cement hydration will influence the internal relative humidity development of early-age concrete (Wei et al. 2016a), the Fick law is used to describe the moisture diffusion process within the concrete:

$$\frac{\partial H}{\partial t} = \nabla \cdot [D(H) \cdot \nabla H] - \frac{\partial H_s}{\partial t} \tag{1}$$

where H is the concrete relative humidity; H_s is the relative humidity due to self-desiccation, which can be obtained from the measured relative humidity result of a sealed concrete specimen; $D(H)$ is the diffusion coefficient as a function of concrete relative humidity, which can be expressed as (Bažant and Najjar 1972)

$$D(H) = D_0 \times \left\{ \alpha + \frac{1 - \alpha}{1 + [(1 - H)/(1 - H_c)]^\beta} \right\} \tag{2}$$

where D_0 is the maximum value of $D(H)$ when $H = 100\%$; α is the ratio of the minimum to the maximum values of $D(H)$; H_c is the concrete relative humidity when $D(H) = 0.5D_0$; β is the parameter characterizing the extent of the drop of $D(H)$ vs. H curves.

The drying surface condition of concrete exposed to environment is defined by the following boundary condition (Kim and Lee 1999):

$$-D(H) \frac{\partial H}{\partial n} = \lambda(H - H_{env}) \tag{3}$$

where H_{env} is the environmental relative humidity; $\frac{\partial H}{\partial n}$ denotes the relative humidity gradient in direction n of the drying surface; λ is the surface diffusion coefficient.

In this study, the user subroutine UMATHT in the heat analysis of ABAQUS is used to simulate the moisture diffusion process because this subroutine can define not only the diffusion coefficient as a function of relative humidity for the external drying process, but also the drop of relative humidity over time caused by the self-desiccation of concrete.

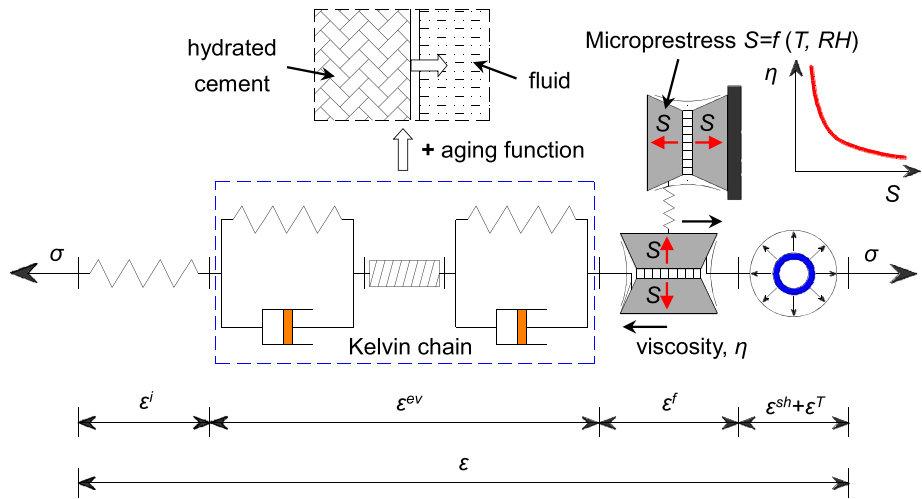


Fig. 1 Rheological scheme of the microstress-solidification theory-based concrete creep model

2.2 Incorporating MPS theory-based creep model into finite element analysis

In the quasi-static structural analysis, the creep property of concrete exposed to the environment was characterized by the microstress solidification (MPS) theory-based creep model (Bažant et al. 1997, 2004). The reason we chose the MPS theory-based creep model is that it can take the effects of both relative humidity and temperature on concrete creep into consideration (Jirásek and Havlásek 2014; Wei et al. 2016b).

In the MPS theory-based model (Bažant et al. 1997, 2004), the mechanics of concrete can be explained by the solidification theory and the microstress theory. In the solidification theory, the volume fraction increase of the non-aging hydration products will result in creep aging phenomenon. While the microstress theory is introduced to account for the temperature and relative humidity effects. Microstress is assumed to be the normal stress acting across the slip planes represented by the hindered adsorbed layers in the nanostructure of cement paste. Microstress relaxes over time and causes concrete creep under constant temperature and relative humidity conditions. However, changes in temperature and relative humidity create an imbalance in microstress, which can reduce the bonding between the microstructure layers and thus increase the creep rate.

To facilitate numerical calculation, the total strain ϵ of concrete under the sustained stress σ can be expressed as the sum of the instantaneous strain ϵ^i , the viscoelastic strain ϵ^{ev} , the purely viscous strain ϵ^f , the shrinkage strain ϵ^{sh} , and the thermal strain ϵ^T , which is illustrated in Fig. 1. And thus, the total strain can be expressed as (Bažant et al. 1997):

$$\epsilon = \epsilon^i + \epsilon^{ev} + \epsilon^f + \epsilon^{sh} + \epsilon^T \tag{4}$$

The instantaneous strain ϵ^i , which is induced immediately after applying the uniaxial stress, can be written as

$$\epsilon^i = q_1 \sigma \tag{5}$$

where q_1 is age independent and does not vary with ages under a certain temperature range.

The viscoelastic strain ε^{ev} is assumed to originate in the calcium silicate hydrate gel, which can be written as

$$\dot{\varepsilon}^{ev}(t) = \frac{\dot{\gamma}(t)}{v(t)} \tag{6}$$

where $\gamma(t) = \int_0^t \Phi(t - \tau)\dot{\sigma}(\tau) d\tau$ is the viscoelastic strain in the hydrate gel, $\Phi(t - t') = q_2 \ln(1 + \xi^n) = A_0 + \sum_{i=1}^N A_i [1 - \exp(-\frac{t-t'}{\tau_i})]$, $\xi = (t - t')/\lambda_0$, $\lambda_0 = 1d$, $\tau_1 = 10^{-4}d$, $\tau_i = 10\tau_{i-1}$ ($i = 2, 3, \dots, 10$), $A_0 = 0.2794q_2$, $A_i = 0.2072 \frac{(3\tau_i)^{0.1}}{1+(3\tau_i)^{0.1}} q_2$ ($i = 1, 3, \dots, 10$); $v(t)$ is the volume fraction of hydration products, which causes the viscoelastic strain of concrete only partially recoverable, $v(t)^{-1} = (\lambda_0/t)^m + \alpha_c$, $\alpha_c = q_3/q_2$, $n = 0.1$, $m = 0.5$.

The viscous strain is completely non-recoverable, which can be modeled by a dashpot and formulated as

$$\dot{\varepsilon}^f(t) = \frac{\sigma(t)}{\eta(S)} \tag{7}$$

where $\eta(S)$ is viscosity of the dashpot and expressed as a power function of micro-prestress S , $\eta(S) = \frac{1}{cbS^{b-1}}$, $b = 2$.

The evolution of micro-prestress can be assumed to follow a Maxwell-type rheological model:

$$\frac{\dot{S}(t)}{C_s} + \frac{S(t)}{\eta(S)} = \frac{\dot{s}(t)}{C_s} \tag{8}$$

where $\frac{\dot{s}(t)}{C_s}$ is the time rate of Maxwell model strain.

To predict the time-dependent deflection of concrete beam caused by creep behavior, a constitutive relation considering the creep and shrinkage properties of concrete in the quasi-static structural analysis should be provided. In this study, since the temperature during all the measurements is controlled nearly constant, the temperature effect on the concrete creep is not considered. With the assumption that the elastic strain, creep strain, and the shrinkage strain are independent of each other, the three-dimensional relationship between the stress increment tensor ($\Delta\sigma_{n+1}$) and the strain increment tensor ($\Delta\epsilon_{n+1}$) can be expressed as Eq. (9):

$$\Delta\sigma_{n+1} = E^{eff} \mathbf{Q}^{-1} \left[\Delta\epsilon_{n+1} - \sum_{i=1}^{10} \frac{(1 - \lambda_i^n)(A_i\sigma_n - \gamma_n^i)}{v_{n+0.5}} - \frac{\psi_{n+0.5}\Delta t_{n+1}}{\eta_{n+0.5}} - \Delta\epsilon_{n+1}^{sh} \right] \tag{9}$$

where σ_n is the stress tensor at time t_n ; Δt_{n+1} is the time increment; E^{eff} is the effective elastic modulus, and $E^{eff} = \frac{1}{q_1 + A_0 + A^{ev} + A^f}$, $A^{ev} = \frac{A_0 + \sum_{i=1}^{10} A_i(1 - \lambda_i^n)}{v_{n+0.5}}$, $A_0 = 0.2794q_2$, $A_i = 0.2072 \frac{(3\tau_i)^{0.1}}{1+(3\tau_i)^{0.1}} q_2$ ($i = 1, 3, \dots, 10$), $\tau_1 = 10^{-4}d$, $\tau_i = 10\tau_{i-1}$ ($i = 2, 3, \dots, 10$), $v_{n+0.5}^{-1} = (\lambda_0/t_{n+0.5})^m + \alpha_c$, $\alpha_c = q_3/q_2$, $n = 0.1$, $m = 0.5$, $A^f = \frac{\psi_{n+0.5}\Delta t_{n+1}}{\eta_{n+0.5}}$; $\eta_{n+0.5} = \eta(S_{n+0.5}) = \frac{1}{2cS_{n+0.5}}$, $S_{n+0.5}$ is the micro-prestress at time $t_{n+0.5}$, which can be determined by $\dot{S} + \psi_S c_0 S^2 = k_1 |\dot{T} \ln(H) + T \frac{\dot{H}}{H}|$, $c_0 = 2c/q_4$, $\psi_{n+0.5}$ is the adjusting factor of the relaxation rate at time $t_{n+0.5}$; $\gamma_n^i = k_n^i \gamma_{n-1}^i + A_i(1 - k_n^i)\sigma_{n-1} + A_i(1 - \lambda_n^i)\Delta\sigma_n$, $k_n^i = \exp(-\Delta\gamma_n^i)$, $\lambda_n^i = (1 - k_n^i)/\Delta\gamma_n^i$, $\Delta\gamma_n^i = \Delta t_n^e/\tau_i$, Δt_n^e is the effective time increment; $\Delta\epsilon_{n+1}^{sh} = k_a(\Delta H_{n+1}, \Delta H_{n+1}, \Delta H_{n+1}, 0, 0, 0)^T$ is the shrinkage strain increment tensor, k_a is the shrinkage coefficient, which denotes the shrinkage strain increment caused by the unit

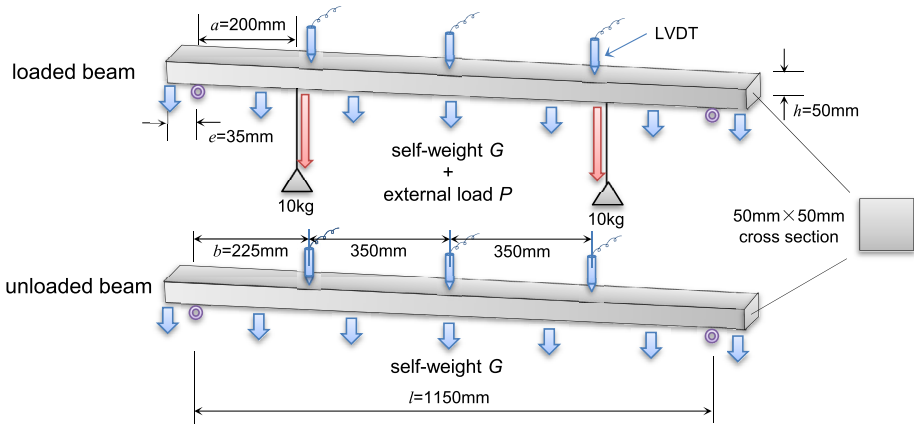


Fig. 2 Schematic illustration of the flexural creep test set-up

RH increment;

$$Q = \begin{bmatrix} 1 & -V & -V & 0 & 0 & 0 \\ -V & 1 & -V & 0 & 0 & 0 \\ -V & -V & 1 & 0 & 0 & 0 \\ 0 & 0 & 0 & 2(1+V) & 0 & 0 \\ 0 & 0 & 0 & 0 & 2(1+V) & 0 \\ 0 & 0 & 0 & 0 & 0 & 2(1+V) \end{bmatrix},$$

V is the Poisson ratio of concrete. $q_1, q_2, q_3, q_4, c,$ and k_1 are the parameters of the MPS theory-based creep model, which can be determined by matching the predicted creep-induced deflection to the measured one, as illustrated in Sect. 4.2.

The user subroutine UMAT in the quasi-static structural analysis is used to define the relationship between the stress increment and the strain increment by incorporating the MPS theory-based creep model and the relationship between the shrinkage strain increment and the RH increment. In the quasi-static structural analysis, the relative humidity results can be extracted from the previous analysis by using the term TEMP in the user subroutine UMAT.

2.3 Experimental design to measure creep-induced deflection

Beam deflection test and exposure condition The flexural creep test set-up was designed in this study to measure the creep-induced deflection of concrete beams. The test uses a four-point bending configuration as shown in Fig. 2. Concrete beams with dimension of 50 mm in height, 50 mm in width, and 1220 mm in length, under the conditions of loaded (self-weight + external load) and unloaded (self-weight only), were measured by their deflection using LVDTs with the precision of 1 μ m. The measuring locations were at the midspan and the 350 mm from the mid-span. The beam deflection in this study is defined as the difference between the recorded data of the LVDT located at the midspan and the average result of the other two LVDTs. This deflection is designed to reduce the negative effect from the disturbance of the beam supports. During the test, the loaded beam was subject to two loads of 10 kg symmetrically about the midspan of the beam, the loading positions were 200 mm away from the beam supports.

Table 2 Mixture proportions and mechanical properties of concrete

Index	Parameters		
Mixture proportions	<i>w/c</i> ratio		0.4
	Cement (kg/m ³)		698
	Water (kg/m ³)		279
	Coarse aggregate (kg/m ³)		795
	Sand (kg/m ³)		530
Mechanical properties	Elastic modulus (GPa)	1 d	17.0
		7 d	29.5
		28 d	31.8
	Flexural strength (MPa)	7 d	3.20

The time-dependent deflection of the loaded beam is mainly caused by the external load as well as the self-weight of the beam, whereas the time-dependent deflection of the unloaded beam is caused only by the self-weight. According to the classical beam theory (Bauchau and Craig 2009), the combination of the external load and the self-weight is expected to produce a maximum tensile stress (calculated according to Eq. (10)) below 50% of the flexural strength of the concrete beam, which will cause little damage on concrete beam and the nonlinear creep behavior will be avoided during the measurement (Ranaivomanana et al. 2013b).

$$\sigma_{\max} = \frac{Pa + \frac{1}{8}Gl^2 - \frac{1}{2}Ge^2}{M_R} \tag{10}$$

where σ_{\max} is the maximum tensile stress caused by the external load P (98 N) and the self-weight G (60 N/m); a is the distance between the support and the external loads (200 mm); l is the distance between supports (1150 mm); e is the cantilever length (35 mm); M_R is the moment of resistance of the beam section ($2.08 \times 10^4 \text{ mm}^3$).

Portland cement was used as cementitious material in concrete. The water-to-cement (*w/c*) ratio of concrete was 0.4. Crushed limestone with the maximum size of 12.5 mm was used as coarse aggregate, which can ensure that the measured results from the beam used in this study reflect the homogeneous property of concrete (Wei et al. 2017). The fine aggregate was natural sand with fineness modulus of 2.6. The mixture proportions and the mechanical properties of this concrete are shown in Table 2.

To assess the effect of internal and external relative humidity on concrete creep, the beams were designed to exposed to two drying conditions: sealed and symmetric drying with top and bottom surfaces exposed to 40% environment relative humidity. All the concrete beams were sealed cured by sealing all surfaces with three layers of self-adhesive aluminium foils until the age of 7 days. For the sealed case, the beams were kept sealed by three layers of self-adhesive aluminium foil on all surfaces during the creep measurement, while for the drying case, the surfaces were exposed to the environment with relative humidity of $40 \pm 5\%$ starting from the age of 7 days. All beam deflection tests started at the age of 7 day and the measuring duration was about 40 days. Each measurement was repeated twice and the average was reported.

Relative humidity and shrinkage measurements To calibrate the diffusion model and to establish the relationship between the relative humidity and the shrinkage, the relative humidity and the shrinkage deformation of the concrete specimens under the sealed condition

and the condition with the top surface exposed to drying at the age of 7 days and 28 days were measured on 1000 mm × 100 mm × 38 mm prism specimens by shrinkage rig. During the measurements, the environmental relative humidity and the temperature were controlled at $40 \pm 5\%$ and $23 \pm 2^\circ\text{C}$, respectively. A LVDT with the precision of $1\ \mu\text{m}$ was used to measure the shrinkage deformation. At the same time, the internal relative humidity of concrete was measured at the middle depth of the specimen by using relative humidity sensors with the precision of 1.8%. The tests were initiated after final set time. More details of the measurement of the internal relative humidity and the shrinkage deformation can be found in our previous work (Wei et al. 2016c). Two specimens were measured for each case and the average was reported.

3 Results

3.1 Creep-induced deflection development of concrete beams exposed to different drying conditions

Figures 3(a) and 3(b) show the measured development of the creep-induced deflection of concrete beams under the sealed and symmetric drying condition, respectively. It is seen that both the loaded and the unloaded beams exhibit an increase of the creep-induced deflection with time. These time-dependent deflections are mainly caused by concrete creep instead of the moisture warping, since concrete shrinkage would introduce a negligible deflection to the concrete beams under the conditions of sealed and symmetric drying. Moisture warping is mainly caused by nonsymmetric drying that a moisture gradient exists along the depth of concrete members, and thus a shrinkage gradient and the consequent warping forms. For the same loading condition, deflection under drying is greater than that under the sealed condition, suggesting that drying would increase the creep deformation of concrete.

The deflection of the loaded beam is much greater than that of the unloaded beam (Figs. 3(a), 3(b)), which is reasonable because the measured deflection of the loaded beam is

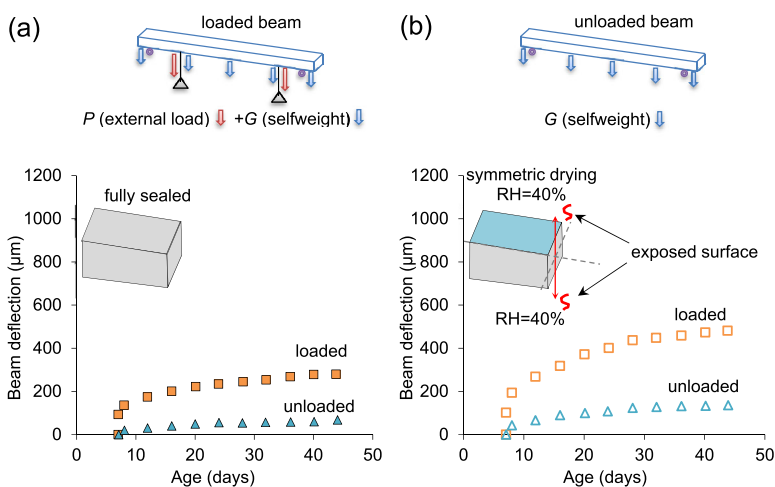


Fig. 3 Measured deflection development of concrete beams under (a) sealed curing, and (b) symmetric drying conditions starting at the age of 7 days

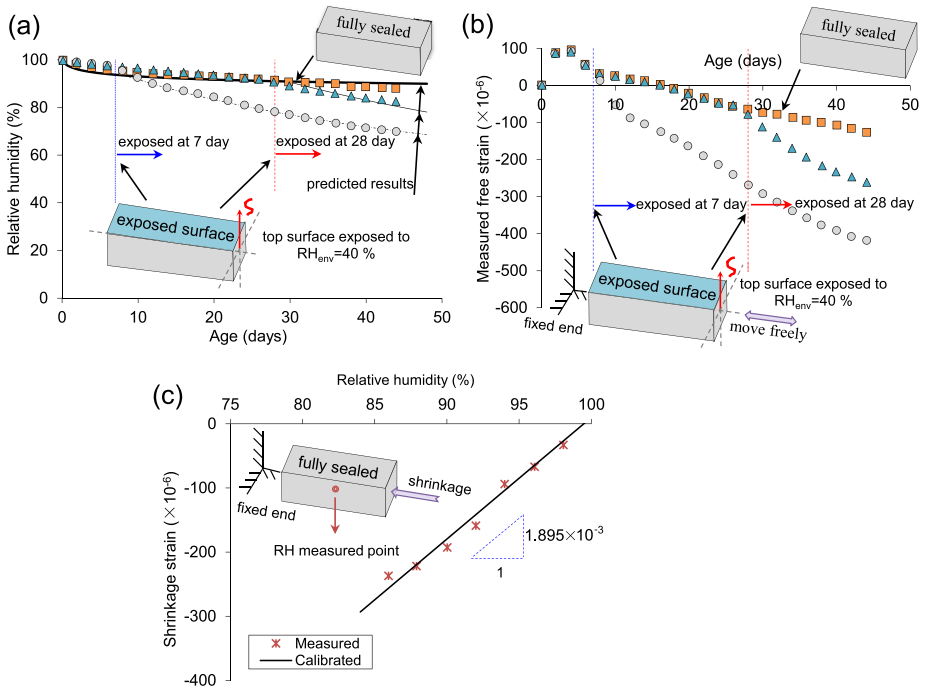


Fig. 4 (a) Measured and predicted relative humidity development, (b) measured free strain development in concrete under different drying conditions: sealed, and exposed to drying at the age of 7 day and 28 day following sealed curing, and (c) relationship between the shrinkage strain and the relative humidity

the time-dependent deflection induced by both the external load and the self-weight. However, the measured deflection of the unloaded beam is the time-dependent deflection caused by the self-weight alone. It should be noted that greater deflection does not mean greater creep, the same set of creep parameters can be used to predict the creep-induced deflections for different loading and drying conditions, as illustrated later in this study.

3.2 Quantifying relationship between relative humidity and shrinkage of concrete

Figure 4 displays the measured relative humidity development in concretes under the sealed condition and the condition with the top surface exposed to drying at the age of 7 days and 28 days after sealed curing. It is seen that under the sealed condition, the relative humidity of concrete decreases with time, which is caused by the self-desiccation of concrete. As expected, the drop of relative humidity is pronounced once the top surface of the specimen is exposed to drying whether it is at the age of 7 days or 28 days.

Figure 4(b) shows the measured shrinkage development in concretes under the sealed condition and the condition with the top surface exposed to drying at the age of 7 days and 28 days after sealed curing. It is seen that all the specimens experience expansion deformation during the very early stage due to the temperature rise caused by the heat released from the hydration of cement, then the specimens shrink mainly due to the drop of relative humidity within the specimens. The development of shrinkage deformation shows a similar trend to that of the relative humidity, indicating that there exists a strong correlation between the relative humidity and the shrinkage deformation of concrete.

Figure 4(c) displays the relationship between the free shrinkage strain and the relative humidity. The results of the sealed concrete were used to establish this relationship, because the strain and the relative humidity are unique and uniform along the cross-section of the sealed concrete specimen. The measured strain is the real strain in concrete, which is not local relative humidity-dependent. It is seen that the shrinkage strain increases nearly linearly with decreasing relative humidity, which is consistent with the existing findings (Bissonnette et al. 1999; Hou et al. 2010; Wei et al. 2011). By a linear regression analysis of the relation between the shrinkage strain and the relative humidity of the sealed specimen, the shrinkage coefficient k_a is determined as 1.895×10^{-3} for concrete used in this study, which can be used to calculate the shrinkage strain of the concrete caused by change of relative humidity in the numerical analysis.

4 Modeling creep-induced deflection considering relative humidity effect

4.1 Predicting relative humidity in concrete exposed to different drying conditions

The first step of the creep-induced deflection modeling is to determine the relative humidity field of the concrete beams exposure to different drying conditions. Prior to relative humidity prediction, it is key to calibrate the parameters in moisture diffusion model as described in Sect. 2.1. The relative humidity developments in shrinkage specimens under the sealed condition and the condition with top surface exposed to drying at the age of 7 days (Fig. 4) were used to calibrate the moisture diffusion model. Then the calibrated moisture model will be validated by the measured relative humidity under the condition with top surface exposed to drying at the age of 28 days. The DC3D8 element with the size of $2 \times 2 \times 2$ mm was used to mesh the $1000 \text{ mm} \times 100 \text{ mm} \times 38 \text{ mm}$ specimen in the modeling. For the specimen with the top surface exposed to drying condition, the surface diffusion coefficient at the drying surface and the environmental humidity were defined in the film condition module. For the specimen under the sealed condition, no film condition was defined such that there is no moisture exchange between the specimen and the environment. The initial relative humidity of the specimen and the environment relative humidity were set as 100% and 40%, respectively. The time increment during the moisture diffusion simulation is set as 0.1 day. Since the experiment temperature was controlled at about $23 \text{ }^\circ\text{C}$ during all the measurement in this study, the temperature was assumed to be constant during the moisture diffusion analysis, which is expected to have minor effect on the simulation. After the calculation, one could obtain the predicted development of the relative humidity at different depths of the specimens.

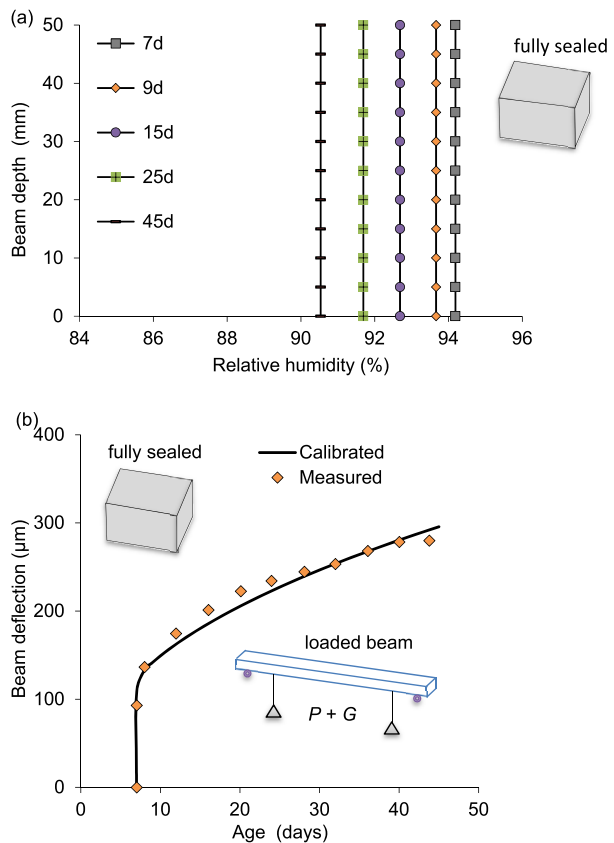
The calibrated parameters of the moisture diffusion model are shown in Table 3 and the predicted relative humidity is plotted as lines shown in Fig. 4(a). It is seen that the predicted relative humidities are in good agreement with the measured ones well.

Figure 5(a) and 7(a) present the predicted distributions of relative humidity along the beam depth for concretes under the sealed and drying conditions at typical ages. As expected, the sealed beam exhibits a uniform RH distribution at all time (Fig. 5(a)). Whereas the RH distribution is nonuniform along the beam depth in the drying case (Fig. 7(a)), which suggests that the local creep property in the drying beam would vary with the position. It is also clear from Figs. 5(a) and 7(a) that the relative humidity distribution is symmetrical about the neutral plane of the beam for sealed and the symmetric drying conditions, which indicates that the shrinkage strain has minor effect on the measured deflection of concrete beam because moisture warping is not occurring in such beam.

Table 3 Calibrated parameters in the moisture diffusion model and the MPS theory-based creep model for concrete tested in this study

Diffusion model		MPS creep model	
Parameter	Value	Parameters	Value
D_0 ($\times 10^{-5}/(m^2/d)$)	9.23	q_1 ($\times 10^{-6}/MPa$)	8.2
α	0.048	q_2 ($\times 10^{-6}/MPa$)	61.3
β	1.1	q_3 ($\times 10^{-6}/MPa$)	39.2
H_c	0.980	q_4 ($\times 10^{-6}/MPa$)	13.7
λ (m^2/d)	0.014	c ($\times 10^{-14}/MPa^2/day$)	6.7
		k_1 (MPa/K)	3.4

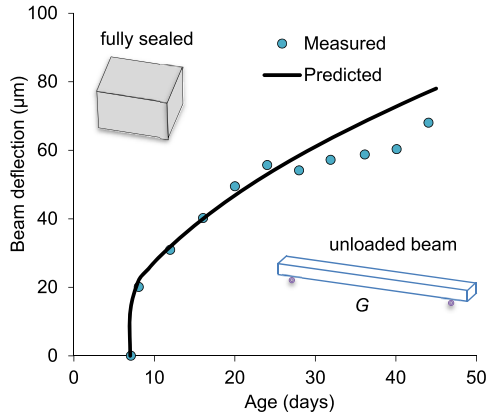
Fig. 5 (a) Predicted relative humidity distribution along the beam depth at typical ages under sealed condition, and (b) measured deflection of loaded beams under sealed condition for calibrating the MPS creep model to obtain the creep parameters in Table 3



4.2 Obtaining creep parameters by calibrating the measured creep-induced deflection of loaded beam under sealed condition

The sequential coupled hygromechanical analysis was conducted on the loaded beams under the sealed condition to obtain the creep property characterized by the MPS theory-based creep model in this study. In the quasi-static structural analysis of the deflection of the loaded beam under the sealed condition, the C3D8 element with the same size as that of the DC3D8 element in the moisture diffusion analysis was used to mesh the concrete beam. The external load and the self-weight were applied to the concrete beam at the age of 7 days.

Fig. 6 Validation of the creep parameters in Table 3 by predicting the creep-induced deflection of unloaded beams under sealed condition



The MPS theory-based creep model was then calibrated by matching the measured creep-induced deflection with the predicted one to obtain the creep parameters. The calibration is conducted through the least square method. The comparison of the measured and the predicted creep-induced deflections of the loaded beams under the sealed condition is shown in Fig. 5(b). It is seen that the predicted deflection match the measured one well, suggesting that the MPS theory-based creep model is capable of characterizing the creep property of concrete subject to bending in addition to characterizing the creep under axial tension and compression loading. The calibrated creep parameters are summarized in Table 3. These parameters will be used in Sects. 4.3–4.6 to predict the creep-induced deflection of beams exposed to other loading and drying conditions for validation of the creep parameters.

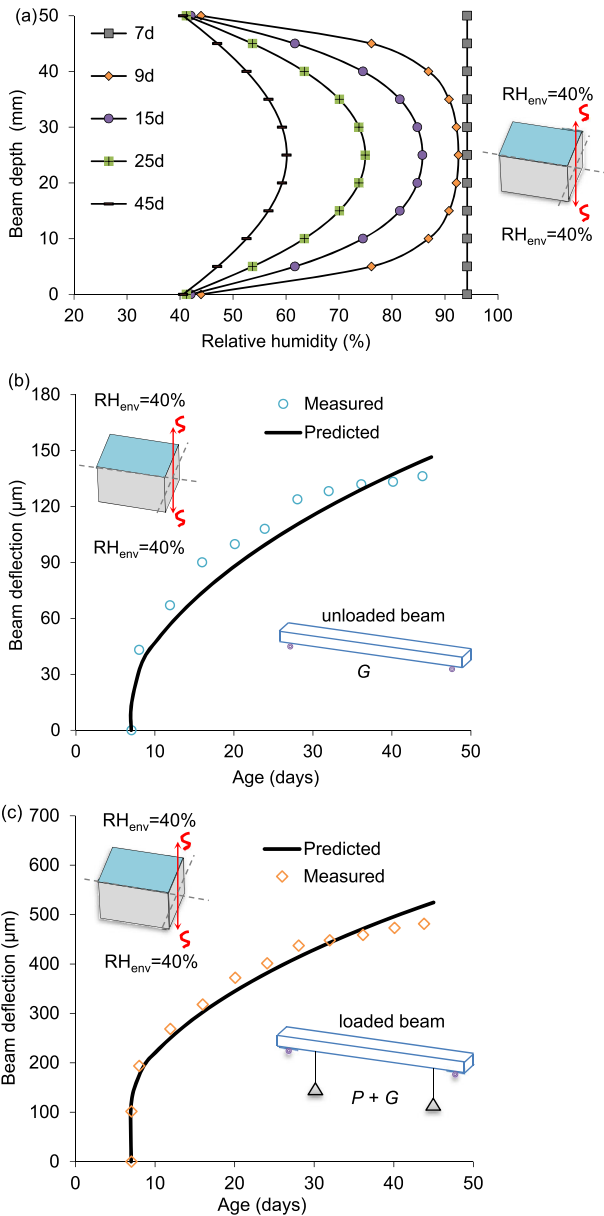
4.3 Predicting creep-induced deflection of unloaded beam under sealed conditions

The calibrated parameters of the MPS model were then used to model the time-dependent deflection of the unloaded concrete beam under the sealed condition. The procedure of the prediction of deflections of the unloaded concrete beam under the sealed condition is similar to that of the loaded beam under the sealed condition. It can be seen from Fig. 6 that the predicted deflection of the unloaded concrete beam under the sealed condition can match the measured one well. It should be noted that the parameters in Table 3 are obtained from a sealed and loaded beam, and the results in Fig. 6 represent the response of the unloaded beam under the sealed condition, the creep deflection of the unloaded beam is induced by the self-weight alone. This indicates that the creep parameters shown in Table 3 will not be influenced by the loading condition (self-weight alone vs. self-weight + external load).

4.4 Predicting creep-induced deflection under symmetric drying conditions

In this section, the measured deflections of the loaded and the unloaded concrete beams with the top and bottom surfaces exposed to the environment will be used to verify whether the creep parameters (shown in Table 3) obtained from the sealed beam test apply to predicting the creep-induced deflection of beams exposure to other loading and drying conditions. The predicted relative humidity of the symmetrically dried beam is shown in Fig. 7(a), and the predicted beam deflection of the unloaded and the loaded beams are shown in Figs. 7(b) and 7(c), respectively.

Fig. 7 (a) Predicted relative humidity distribution along the beam depth at typical ages under the conditions of symmetric drying, and validation of the creep parameters in Table 3 by predicting the creep-induced deflection of (b) unloaded and (c) loaded beams exposed to symmetric drying at the age of 7 day



It can be seen from Fig. 7 that the measured creep-induced deflection of the loaded and the unloaded concrete beams with top and bottom surfaces exposed to drying can be well captured by the predicted ones based on the creep parameters shown in Table 3. This confirms that the stress level or the relative humidity will not affect the creep property within the linear creep range, which depends only on the mixture proportions of concrete.

The results shown above suggest that the creep property obtained from concrete deflection in this study is intrinsic; it does not depend on the experimental loading and drying conditions. The calibrated moisture diffusion model and MPS theory-based creep model

will be used to predict the beam deflection under other drying conditions in the following sections.

4.5 Predicting creep-induced deflection of concrete beam exposed to different environmental relative humidities

The relative humidity development and the deflection development of the loaded concrete beam with top and bottom surfaces exposed to the drying environment with RH of 40%, 60%, and 80% will be predicted in this section. This is done through the sequential coupled hygro-mechanical finite element analysis by employing the calibrated moisture diffusion model and MPS theory-based model shown in Table 3. Figure 8 shows the development of the predicted relative humidity within the concrete beam. It can be seen that the RH distributions along the beam depth are similar for different drying condition with RH of 40%, 60%, and 80%, i.e., they are symmetric about the neutral plane of the concrete beam. Therefore, the beam deflection caused by concrete shrinkage induced by the change of RH is expected to be negligible. Besides, it can be seen from Fig. 8 that the lower the environmental RH, the longer time is required for the concrete beam to reach moisture equilibrium.

Figure 9 shows the beam deflection development of concrete beam with top and bottom surfaces exposed to environmental RH of 40%, 60%, and 80%. It is seen that the lower the environmental relative humidity, the larger deflection the concrete beam exhibits. This implies that concrete creeps more at a lower environmental relative humidity, which is reasonable and is consistent with the existing experimental findings (Pickett 1942; Rossi et al. 2013; Cagnon et al. 2015). The predicted results shown in Fig. 9 indicate that the creep property of concrete can be reasonably predicted by the numerical method in this study.

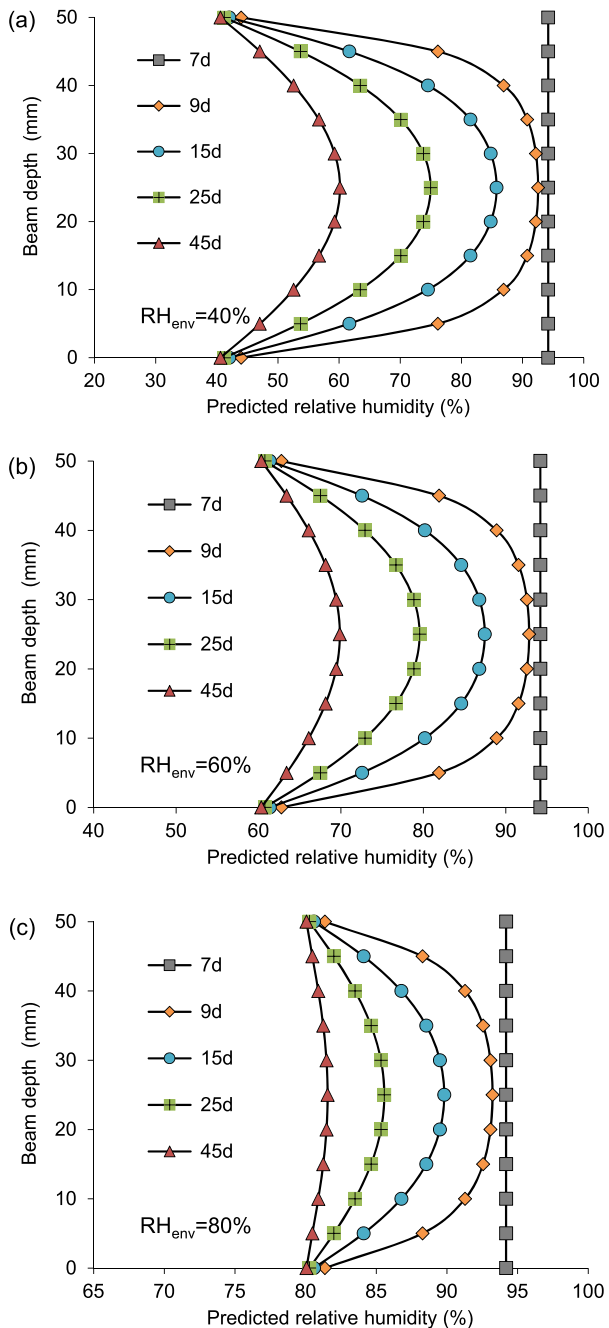
4.6 Predicting creep-induced deflection of concrete beam with different surfaces exposed to drying

The drying surface of concrete can affect the relative humidity within concrete specimen, thus will influence the creep development of concrete specimen, which will be verified in this section. Figure 10 shows the deflection of concrete beam with three different drying cases, i.e., with top and bottom surfaces exposed to environmental RH of 40%, with left and right surfaces exposed to environmental RH of 40%, and with all the lateral surfaces exposed to environmental RH of 40%. As can be seen in Fig. 10, the beam deflections of the three cases with different surface exposed to drying are slightly different from each other. For example, the beam deflection at the age of 45 days with top and bottom surfaces exposed to drying is 4% larger than that with all the lateral surfaces exposed to drying, while the beam deflection at the age of 45 days with left and right surfaces exposed to drying is 9% larger than that with all the lateral surfaces exposed to drying. The main reason lies in the fact that the relative humidities within concrete beams for these three cases are different, which will result in different creep development, i.e., different beam deflection.

5 Conclusions

It is critical to consider the effect of relative humidity on creep behavior of concrete members. In this study the creep-induced deflection was investigated both experimentally and numerically on concrete beams exposed to sealed and symmetric drying conditions. The major conclusions can be drawn as follows:

Fig. 8 Predicted relative humidity distribution along the beam depth at typical ages when the top and bottom surfaces of concrete beam are exposed to environmental relative humidity of (a) 40%, (b) 60%, and (c) 80%



1. An experimental method was proposed to measure the creep-induced deflection of concrete beam to study the intrinsic creep of concrete under different drying conditions without involving the shrinkage effect. This experimental method avoids the involvement of drying-related shrinkage during the creep strain measurement which is normally encoun-

Fig. 9 Predicted creep-induced deflection of the loaded concrete beam when its top and bottom surfaces are exposed to environmental relative humidity of 40%, 60%, and 80%

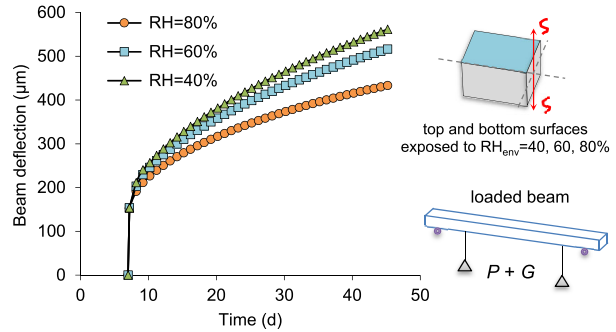
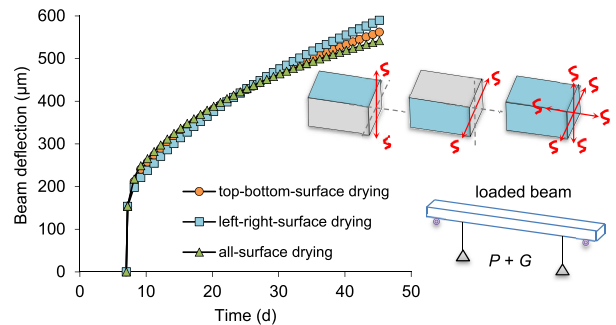


Fig. 10 Predicted creep-induced deflection of the loaded concrete beam with different surfaces exposed to environmental relative humidity of 40%



tered during the conventional creep testing, especially the surface measurement of creep strain on a concrete specimen where a differential shrinkage gradient exists.

- The creep parameters of concrete were derived from the measured deflection results through the numerical method proposed in this study. The numerical method was conducted by the sequential coupled hydromechanical finite element analysis on concrete members incorporating the microprestress solidification theory-based creep model. The parameters were then validated by the measured creep-induced beam deflections. It was found that the creep parameters can be used to predict the creep-induced deflection of concrete beams under different loading (loaded vs. unloaded) and drying conditions (sealed and symmetric drying). The creep parameters are materials-dependent only, they can be used to predict creep behavior of concrete members without considering drying-related size effect.
- The microprestress solidification (MPS) theory-based creep model can capture the creep-induced deflection development of concrete beams under both sealed and drying conditions very well by considering the relative humidity effect. It should be noted that the temperature variation was not considered in measuring and modeling creep by the method proposed in this study, future investigation is needed to consider simultaneously the temperature and relative humidity effects.

Acknowledgement The authors wish to thank for the support from National Natural Science Foundation of China under Grant Nos. 51578316 and 51778331.

Publisher's Note Springer Nature remains neutral with regard to jurisdictional claims in published maps and institutional affiliations.

References

- ACI Committee: Guide for modeling and calculating shrinkage and creep in hardened concrete. ACI Committee 209 (2008)
- Acker, P., Ulm, F.J.: Creep and shrinkage of concrete: physical origins and practical measurements. *Nucl. Eng. Des.* **203**(2), 143–158 (2001)
- Bauchau, O.A., Craig, J.I.: Euler-Bernoulli beam theory. In: *Structural Analysis*, pp. 173–221. Springer, Houten, Netherlands (2009)
- Bažant, Z.P., Najjar, L.J.: Nonlinear water diffusion in nonsaturated concrete. *Mater. Struct.* **5**(1), 3–20 (1972)
- Bažant, Z.P., Xi, Y.: Drying creep of concrete: constitutive model and new experiments separating its mechanisms. *Mater. Struct.* **27**(1), 3–14 (1994)
- Bažant, Z.P., Hauggaard, A.B., Baweja, S., et al.: Microprestress-solidification theory for concrete creep. I: Aging and drying effects. *J. Eng. Mech.* **123**(11), 1188–1194 (1997)
- Bažant, Z.P., Cusatis, G., Cedolin, L.: Temperature effect on concrete creep modeled by microprestress-solidification theory. *J. Eng. Mech.* **130**(6), 691–699 (2004)
- Bissonnette, B., Pierre, P., Pigeon, M.: Influence of key parameters on drying shrinkage of cementitious materials. *Cem. Concr. Res.* **29**(10), 1655–1662 (1999)
- Cagnon, H., Vidal, T., Sellier, A., et al.: Drying creep in cyclic humidity conditions. *Cem. Concr. Res.* **76**, 91–97 (2015)
- Charron, J.P., Sorelli, L., Frech-Baronet, J.: Creep behavior of cement paste, mortar and concrete: the role of relative humidity and interface porosity. In: *Concreep10*, 21–23 September (2015)
- Ghezal, A.F., Assaf, G.J.: Time-dependent behavior of self-consolidating concrete loaded at early age: influence of chemical admixtures. *J. Mater. Civ. Eng.* **28**(1), 04015066 (2015)
- Hou, D., Zhang, J., Wei, S.: Experimental study on the relationship between shrinkage and interior humidity of concrete at early age. *Mag. Concr. Res.* **62**(3), 191–199 (2010)
- Jirásek, M., Havlásek, P.: Microprestress–solidification theory of concrete creep: reformulation and improvement. *Cem. Concr. Res.* **60**, 51–62 (2014)
- Kim, J.K., Lee, C.S.: Moisture diffusion of concrete considering self-desiccation at early ages. *Cem. Concr. Res.* **29**(12), 1921–1927 (1999)
- Pickett, G.: The effect of change in moisture content on the creep of concrete under a sustained load. *J. Am. Concr. Inst.* **38**, 333–355 (1942)
- Ranaivomanana, N., Multon, S., Turatsinze, A.: Basic creep of concrete under compression, tension and bending. *Constr. Build. Mater.* **38**, 173–180 (2013a)
- Ranaivomanana, N., Multon, S., Turatsinze, A.: Tensile, compressive and flexural basic creep of concrete at different stress levels. *Cem. Concr. Res.* **52**, 1–10 (2013b)
- Rossi, P., Tailhan, J.L., Maou, F.L.: Comparison of concrete creep in tension and in compression: influence of concrete age at loading and drying conditions. *Cem. Concr. Res.* **51**(9), 78–84 (2013)
- Sellier, A., Multon, S., Buffo-Lacarrière, L., et al.: Concrete creep modelling for structural applications: non-linearity, multi-axiality, hydration, temperature and drying effects. *Cem. Concr. Res.* **79**, 301–315 (2016)
- Un, C.H., Sanjayan, J.G., Nicolas, R.S., et al.: Mini-beam test for assessing the creep trend of paste, mortar, and concrete. In: *CONCREEP*, vol. 10, pp. 1350–1359 (2015)
- Wei, Y., Hansen, W., Biernacki, J.J., Schlangen, E.: Unified shrinkage model for concrete from autogenous shrinkage test on paste with and without GGBFS. *ACI Mater. J.* **108**(1), 13–20 (2011)
- Wei, Y., Guo, W., Liang, S.: Microprestress-solidification theory-based tensile creep modeling of early-age concrete: considering temperature and relative humidity effects. *Constr. Build. Mater.* **127**, 618–626 (2016a)
- Wei, Y., Guo, W., Zheng, X.: Integrated shrinkage, relative humidity, strength development, and cracking potential of internally cured concrete exposed to different drying conditions. *Dry. Technol.* **34**(7), 741–752 (2016b)
- Wei, Y., Liang, S., Gao, X.: Numerical evaluation of moisture warping and stress in concrete pavement slabs with different water-to-cement ratio and thickness. *J. Eng. Mech.* **143**(2), 04016111 (2016c)
- Wei, Y., Liang, S., Guo, W.: Decoupling of autogenous shrinkage and tensile creep strain in high strength concrete at early ages. *Exp. Mech.* **57**(3), 475–485 (2017)